

# Leveraging waveform complexity for confident detection of gravitational waves

Jonah B. Kanner

*LIGO Laboratory, California Institute of Technology, Pasadena, CA 91125, USA\**

Tyson B. Littenberg

*Center for Interdisciplinary Exploration and Research in Astrophysics (CIERA) & Department of Physics and Astronomy, Northwestern University, 2145 Sheridan Road, Evanston, IL 60208*

Neil Cornish and Meg Millhouse

*Montana State University, Bozeman, Montana 59717, USA*

Enia Xhakaj

*Lafayette College, 730 High St, Easton, PA 18042*

Francesco Salemi and Marco Drago

*Data Analysis Group, Albert-Einstein-Institut, Max-Planck-Institut fr, Gravitationsphysik, D-30167 Hannover, Germany*

Gabriele Vedovato

*INFN Padova, Via Marzolo 8, Padova I-35131, Italy*

Sergey Klimenko

*University of Florida, Gainesville, FL 32611, USA*

The recent completion of Advanced LIGO suggests that gravitational waves (GWs) may soon be directly observed. Past searches for gravitational-wave transients have been impacted by transient noise artifacts, known as glitches, introduced into LIGO data due to instrumental and environmental effects. In this work, we explore how waveform complexity, instead of signal-to-noise ratio, can be used to rank event candidates and distinguish short duration astrophysical signals from glitches. We test this framework using a new hierarchical pipeline that directly compares the Bayesian evidence of explicit signal and glitch models. The hierarchical pipeline is shown to have strong performance, and in particular, allows high-confidence detections of a range of waveforms at realistic signal-to-noise ratio with a two detector network.

## I. INTRODUCTION

Installation of the Advanced LIGO [1] gravitational wave (GW) detectors has recently been completed, with science operations planned to begin in fall of this year. These new detectors are designed to make detection of GWs a reality. For example, current estimates predict that Advanced LIGO will eventually detect between 1 and 400 binary neutron star mergers per year [2]. A number of other sensitive GW detectors are in various stages of construction and installation, including Advanced Virgo [3], GEO600 [4], and Kagra [5].

The principal analysis challenge in finding transient signals in LIGO data is separating signatures of astrophysical sources from large populations of transient detector artifacts (glitches) in the data. Researchers have demonstrated a variety of search techniques for finding transient signals with initial LIGO and initial Virgo. Searches for specific classes of signals, including binary neutron star mergers and mergers of solar mass black

holes, have demonstrated performance in real LIGO data similar to expectations based on Gaussian noise, suggesting they are optimally sensitive [6]. These searches use a matched filtering technique to reject glitches, an approach which relies on detailed knowledge of the expected waveform.

On the other hand, LIGO data is also searched for generic GW transients, known as GW bursts, which are not constrained by a specific source model. Such searches are designed to detect unmodeled and/or unexpected GW sources. These searches are less constrained by waveform morphology, and so are more sensitive to glitches which diminish detection confidence of potential GW event candidates. For example, past searches for bursts in LIGO data have shown background distributions that included high signal-to-noise ratio glitches [7, 8] which diminish detection confidence of any potential GW events.

One approach to confident Burst detection is to carefully divide the parameter space, and improve detection confidence for particular classes of signals. Recent work by Thrane and Coughlin [9] has shown that searches for long duration bursts, with time-scales greater than several seconds, are insensitive to most glitch populations,

---

\* jkanner@caltech.edu

and so can successfully identify long bursts with high confidence. For short duration searches, it may also be possible to carefully study background distributions, and apply *ad hoc* cuts designed to isolate portions of parameter space that are relatively glitch free.

Taking a different approach, Cornish and Littenberg put forward the **BayesWave** pipeline [10], and described how it uses a novel detection statistic to characterize GW data. Most Burst search algorithms apply selection cuts to remove glitches, and then rank the remaining signals with a statistic proportional to signal-to-noise ratio (SNR). **BayesWave** instead attempts to fit the data with both a GW signal model and an explicit glitch model, and calculate the Bayesian odds ratio between the two competing hypotheses. Because of this, **BayesWave** may be more robust against the high SNR glitches which have been problematic for past searches.

In this work, we describe how **BayesWave** can be used as a second stage to follow-up triggers from a leading burst pipeline, **coherentWaveBurst** (**cWB**) [11], to create a “hierarchical pipeline” that combines the best features of the two tools. To test the performance, we measure the ability of the joint search to detect simulated gravitational waves while rejecting glitches using the two LIGO detectors in Livingston and Hanford. We study the performance on a range of waveforms, including both binary black hole mergers and several *ad hoc* waveforms that have been used in previous burst searches.

## II. THE HIERARCHICAL PIPELINE

The **cWB** pipeline has been used in a number of previous burst searches. The algorithm looks for coherent excess power by cross-correlating data streams between two or more detector sites, using projection coefficients that reject signal power which is inconsistent with a source at a hypothesis sky position. The detection statistic,  $\rho$ , is designed to scale with the SNR of the GW signal. **cWB** has shown excellent performance in several metrics. It can analyze a large amount of data with low computational cost. It is sensitive to GW signals with a large variety of waveforms. It has been shown to be robust to calibration errors and other uncertainties, and it also provides information about the reconstructed parameters of the signal, including an estimate of the sky position, polarization, and waveform. Because  $\rho$  scales with SNR, and **cWB** attempts to search a very broad parameter space, even a small number of coincident, high SNR glitches can make high confidence detections a challenge. To address this, **cWB** uses statistics based on the reconstructed noise energy to distinguish GW signals from glitches. Also **cWB** uses various search strategies to divide the parameter space and single out specific glitch families.

The recently developed **BayesWave** pipeline computes the Bayesian evidence for three competing models: the data contain only Gaussian noise, the data contain an astrophysical signal, or the data contain one or more

glitches. The algorithm uses a Reverse Jump Markov Chain to calculate full posterior distributions for each of these models, and thermodynamic integration to compute the associated evidence. As a detection statistic, we adopt the natural logarithm of the evidence ratio, or “Bayes Factor”, between the signal and the glitch model ( $\log(\mathcal{B}_{S,G})$ ). Because the **BayesWave** detection statistic is derived from a framework that expects glitches in the data, as opposed to assuming Gaussian noise, it may better reflect the true probability that a given candidate is astrophysical in nature. In addition, the algorithm calculates posterior distributions for a number of parameters, including the sky position, central frequency, and bandwidth of any detected event. Such information could aid in astrophysical interpretation. A current limitation of **BayesWave** is that the run time is relatively slow, so that analyzing large data sets is impractical.

The **cWB** detection statistic  $\rho$  is derived from a “maximum likelihood” framework, which calculates an optimal statistic for identifying gravitational wave bursts embedded in Gaussian noise. It is natural, then, that  $\rho$  scales with the signal energy present in the data, since Gaussian noise is extremely unlikely to produce high SNR signals.  $\mathcal{B}_{S,G}$ , on the other hand, is calculated in a framework that directly compares a signal model with a glitch model. Under this assumption, a louder event does not necessarily imply a larger likelihood of an astrophysical origin. Indeed, very loud glitches, with SNRs of order 100, are routinely observed in the LIGO instruments, where the bulk of astrophysical signals are most likely to be at low SNR. Rather, the principal scaling for the **BayesWave** detection statistic can be expressed as [12]:

$$\log \mathcal{B}_{S,G} \sim \mathcal{O}(N \log \text{SNR}) \quad (1)$$

where  $N$  represents the number of sine-gaussian wavelets used to reconstruct the signal. The fact that the detection statistic scales only with the logarithm of the SNR suggests that in this framework, a very loud event does not provide much evidence for the signal model. On the other hand, the detection statistic does show a strong scaling with the complexity of the signal in the time-frequency plane, as represented by  $N$ , the number of wavelets required. This brings out the salient feature that distinguishes **BayesWave** from other Burst pipelines - complexity in signal morphology, rather than SNR, determines the significance of observed events.

For GW signals that require only a single wavelet to reconstruct (*i.e.* sine-gaussian waveforms),  $N \sim 1$ , and we expect the detection statistic to be effectively flat as a function of SNR, since  $\log \mathcal{B}_{S,G}$  will scale slowly as  $\log \text{SNR}$ . On the other hand, for a signal with a non-trivial time-frequency structure (*i.e.* anything *other than* a sine-gaussian), we expect to better resolve the signal with higher SNR, and so require more wavelets, so that

$$N \sim (1 + \beta) \text{SNR} \quad (2)$$

where  $\beta$  depends only on the waveform morphology,  $\beta \geq$

0, and  $\beta$  is larger for waveform morphologies that have complicated time-frequency structure.

In this work, we implement a hierarchical pipeline, where `BayesWave` acts as a follow-up stage, which can amplify the significance of complex GW events identified by `cWB`. This takes advantage of the computational efficiency and robust trigger identification of `cWB`, while leveraging the unique signal-glitch separation capabilities of `BayesWave`. In our scheme, `cWB` was run over a large set of interferometer data, represented in this study by roughly 50 days of data from the last science run of initial LIGO. A nominal threshold was set for  $\rho$ , and for each event above threshold, `BayesWave` was run over 4 seconds of data centered on the trigger time, with the goal of calculating  $\log(\mathcal{B}_{S,G})$  for the 1 second of data around the trigger time. This combined pipeline was run for two different testing scenarios:

- Binary black hole merger waveforms added to rescaled LIGO noise, to emulate the power spectral density of expected noise in the advanced LIGO detectors.
- Ad-hoc waveforms used in previous Burst searches added to initial LIGO data

In the following sections, we describe these two data sets in detail, and present the results of our testing.

### III. TESTING WITH BINARY BLACK HOLE WAVEFORMS

#### A. Data Set

While GW signals from stellar mass black-hole mergers can be best recovered using matched filters, intermediate mass black hole mergers ( $M \sim 100M_{\odot}$ ) may be well detected with burst searches, since the time the source spends in the LIGO frequency band is very short. While matched filtering may still be ideal in many cases, burst searches present the advantage that they are robust against modeling uncertainties. For example, obtaining a template bank of model waveforms is difficult for cases where the black holes have misaligned spins or are on eccentric orbits. Previous studies have compared the performance of burst pipelines and matched filtering pipelines in this regime, and found them to have similar sensitivity [13].

To emulate a search for intermediate mass binary black holes with Advanced LIGO, we used 26.6 days of coincident data from the Hanford and Livingston LIGO detectors from the end of the last science run of initial LIGO, in August-October of 2010. This data was “recoloring” to have a noise power spectral density that mimics roughly what we expect from the first science run of Advanced LIGO, with a 55 Mpc sky-averaged range for binary neutron star mergers [14]. The recoloring process was intended to simulate noise levels from the near future de-

tectors, while preserving the non-gaussian features in the data.

#### B. Background

In order to measure the rate of false-positives found by our hierarchical pipeline, we created 30,000 time-slide data sets by introducing artificial time off-sets between the Hanford and Livingston data streams. This background data represent 1896 years of effective livetime. `cWB` was run over all of this data, searching for transients in a band from 16-512 Hz with an elliptical polarization constraint, similar to the configuration used in [13]. We set a nominal threshold at  $\rho > 8.1$ , yielding 500 background triggers from the time-slide data. All 500 background triggers were processed by `BayesWave` using the same bandwidth as `cWB` to determine the final detection statistic,  $\log(\mathcal{B}_{S,G})$ , for each event. The false alarm rate (FAR) for this background set is shown in Figure 1. The loudest background event has  $\log(\mathcal{B}_{S,G}) \sim 19$ . We also show in Figure 2 the same background set, as a function of the `cWB` detection statistic  $\rho$ . If no additional `cWB` selection cuts are applied, the same FAR may be achieved with a threshold of  $\rho > 107$ . We tried applying both “Category 2” and “Category 3” data quality cuts, as was done in initial LIGO searches [8], and found that this makes no difference for the loudest several events that dominate the “tail” of the `cWB` background (See Figure 2). To address the background problem, the `cWB` trigger set would require additional processing, such as dividing up the parameter space, additional selection cuts, or a follow-up with an additional burst algorithm as described in this work.

A novel feature of the `BayesWave` pipeline is that it allows an *a priori* estimate of the expected background rate, which may be compared with the results of running the hierarchical pipeline. Based on studies of LIGO noise properties [15], we expect coincident glitches in the LIGO detectors roughly every 100 seconds ( $R_{\text{glitch}} = 0.01$  Hz). For glitches that mimic real signals, the Bayes Factor  $\mathcal{B}_{S,G}$  is dominated by the “Occam Factor”, an estimate of the fraction of glitch parameter space that is consistent with the signal model for a given event. This immediately leads to an expectation for the background rate of glitches that mimic real signals by chance,

$$\text{FAR}_{\text{expected}} \sim (1/\mathcal{B}_{S,G}) \times R_{\text{glitch}} \quad (3)$$

which is plotted as a gray dashed line in Figure 1.

#### C. Injections

To test the ability of the joint `cWB` plus `BayesWave` pipeline to recover GW signals, we added two sets of simulated black hole mergers to the data. One set contained waveforms from binary black holes with component masses of 50  $M_{\odot}$ , the other contained component

masses of  $150 M_{\odot}$ . Both sets were distributed uniformly in co-moving volume, and generated using non-spinning effective-one-body waveforms, known as EOBNRv2 [16].

Scatter plots of the recovered injections can be seen in Figures 3 and 4. In each figure, the x-axis corresponds to the `cWB` detection statistic  $\rho$ , while the y-axis shows the `BayesWave` detection statistic  $\log \mathcal{B}_{S,G}$ . As a demonstration that the hierarchical pipeline can make high confidence detections, the blue dashed line in each figure represents the threshold required for a “3- $\sigma$ ” level detection in a year of observations, corresponding to a FAR of  $9 \times 10^{-11}$  Hz. Many injections are seen to be well above this threshold, even with network SNR as low as  $\sim 10$ .

For comparison, the red vertical line shows the  $\rho$  value that would be required for the same confidence level, if only the basic `cWB` cuts were used. The two dashed lines, then, divide the figure into four quadrants which classify each injection as detected by the hierarchical pipeline but not the basic `cWB` cuts (top left), detected by `cWB` but not by the hierarchical pipeline (bottom right), detected by both approaches, or detected by neither. The threshold required by the basic `cWB` cuts is clearly too high to be practical - events would need a network SNR  $> 50$  to stand above the background. Any search with `cWB`, then, would need some additional layer of processing. The events in the top-left quadrant of Figures 3 and 4 represent black hole merger signals which were detected with low-significance by the basic `cWB`, but were “promoted” by the `BayesWave` follow-up. The fact that most of the injections with SNR 10-50 fall in this range suggests that, for these waveforms, the hierarchical pipeline described in this work represents a successful strategy. Moreover, while the blue dashed line corresponds to a  $3\sigma$  detection level, we note that the loudest background event in the data set had a value of  $\log \mathcal{B}_{S,G} \sim 19$ . Many of the events are seen to rank higher than this, suggesting that detections at even higher significance levels are possible, even with plausible SNR values.

To quantify the performance of the hierarchical pipeline for black hole mergers, we follow the methodology described in [13] and plot the “sensitive radius” at a range of FAR values in Figure 5, a statistic that characterizes the effective range of the survey. At very high FAR values ( $\sim 1$  per 10 years), the pipeline presents no advantage over a basic application of `cWB`. However, moving to the left side of the plot, representing high confidence detections, the hierarchical pipeline still detects a large fraction of the injection set. This means that the hierarchical pipeline is able to detect black hole mergers at high confidence, even in the presence of glitches, without reliance on a matched filter technique.

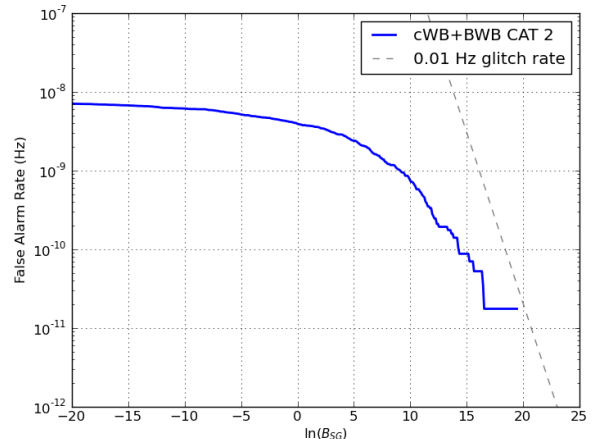


FIG. 1. Background for the hierarchical pipeline in the the recolored data used to study IMBH signals. The background was calculated using 1900 years of time-slide data. The loudest background event has  $\log \mathcal{B}_{S,G} = 19$ . The gray curve shows the expected background, based on the assumption that a glitch appears in the data every 100 seconds.

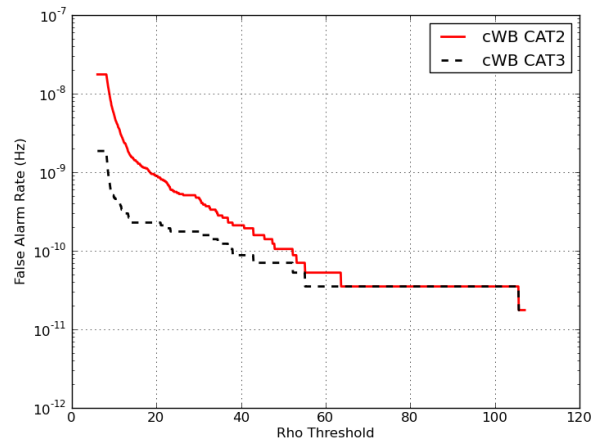


FIG. 2. Background for the `cWB` pipeline in the the recolored data used to study IMBH signals. The background was calculated using 1900 years of time-slide data. The loudest background event has  $\rho = 107$ . The two curves show the background after applications of “Category 2” (red) and “Category 3” (black) data quality vetoes.

## IV. TESTING WITH AD-HOC WAVEFORMS

### A. Data Set

In principle a burst search should be sensitive to a wide range of possible signal morphologies. In order to test this, without reliance on any particular astrophysical models, past all-sky burst searches have made use of a suite of ad-hoc waveforms to measure pipeline per-

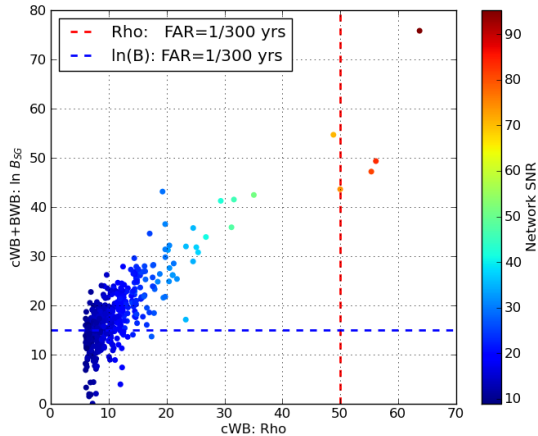


FIG. 3. Scatter plot of two detection statistics with simulated mergers of pairs 50 solar mass black holes, comparing the hierarchical pipeline with the basic `cWB` cuts. The dashed lines correspond to thresholds required for a false positive rate of 1 in 300 years. Injections in the upper-left quadrant were “promoted” by the `BayesWave` follow-up.

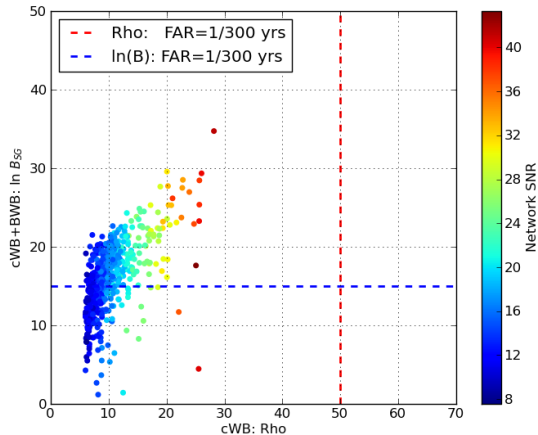


FIG. 4. Scatter plot of two detection statistics with simulated mergers of pairs 150 solar mass black holes, comparing the hierarchical pipeline with the basic `cWB` cuts. The dashed lines correspond to thresholds required for a false positive rate of 1 in 300 years. Injections in the upper-left quadrant were “promoted” by the `BayesWave` follow-up.

formance [8]. This set includes two extremes of waveform complexity. At one extreme, lineally polarized sine-gaussian, or Morlet-Gabor, waveforms represent a minimum possible “time-frequency volume” [17], and so may be described as the simplest possible signals in this domain. They also correspond to the basis functions used by the `BayesWave` pipeline, and so are best represented by a single wavelet ( $N \approx 1$ ). The set also contains unpolarized “white-noise burst” waveforms, which are random waveforms within a fixed duration and bandwidth.

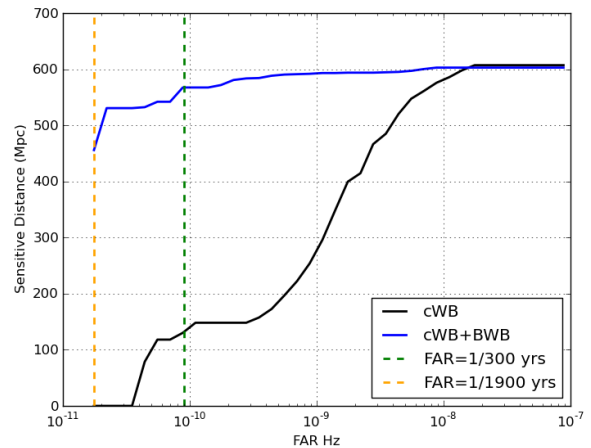


FIG. 5. Sensitive distance for the 50-50 solar mass injections. The sensitive distance is a measure of the effective radius to which the analysis is sensitive. The shown curves apply only category 2 data quality cuts.

In the time-frequency plane, these waveforms essentially fill a large block with edge sizes corresponding to the duration and bandwidth of the signal. The white noise bursts are a very poor match to the `BayesWave` Morlet-Gabor basis, and so require a large number of wavelets to reconstruct. In this sense, they have a very complex time-frequency structure. The unpolarized white-noise bursts also provide an interesting test of the `BayesWave` signal model, which uses an elliptical polarization model for GW signals. To measure the performance of the hierarchical pipeline using these ad-hoc waveforms, we used 51 days of coincident data from the H1-L1 network during the last science run of initial LIGO, between August and October 2010. The data and data quality information are both available through the LIGO Open Science Center [18].

## B. Background

In order to measure the FAR of the search, the data were time-shifted 500 times to create a background set with 70 years of effective livetime. Following [8], we searched through this data set using `cWB` in a bandwidth from 32 to 2048 Hz. As for the black hole merger data set, each trigger from `cWB` above a nominal threshold ( $\rho > 8$ ) was processed in a 1 second window using `BayesWave`. In order to reduce processing time, we used the central frequency as reported by `cWB` to limit the bandwidth of some `BayesWave` jobs. Triggers with a central frequency less than 200 Hz were processed with a bandwidth from 16-512 Hz, while triggers with a higher central frequency used a band from 16-2048 Hz. The rate of background triggers for the hierarchical pipeline is shown in Figure

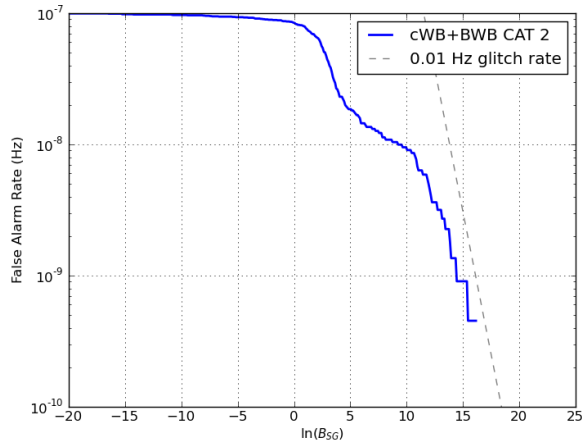


FIG. 6. Background for the hierarchical pipeline using the LIGO data used to study ad-hoc signals. The background was calculated using 70 years of time-slide data. The loudest background event has  $\log \mathcal{B}_{S,G} = 16$ . The gray curve shows the expected background, based on the assumption that a glitch appears in the data every 100 seconds.

6, and the corresponding FAR for the basic application of **cWB** is shown in Figure 7.

The background distributions were broadly similar to the distributions for the recolored data set. In Figure 7, we see that the basic **cWB** cuts lead to a “tail” in the distribution. As in the IMBH data set, we see in Figure 6 that the hierarchical pipeline shows a distribution that is similar to expectations based on the known glitch rate, marked as a grey line in the figure. For this data set, the background represents 70 years of effective livetime, so the detection statistic of the loudest event corresponds to a FAR threshold of  $5 \times 10^{-10}$  Hz.

### C. Injections: white noise bursts

To measure the ability of the hierarchical pipeline to recover astrophysical signals, we added simulated signals to the data set before running the pipeline. Tens of thousands of injections were added to the 51 days of data. As with the background set, this data was searched first with **cWB** to identify triggers with  $\rho > 8$ . Unlike with the background set, for the injections we randomly selected a sub-set of around 200 of the **cWB** triggers for each waveform to process with **BayesWave**.

We tested three different white noise burst waveforms with short duration ( $t < 0.1$  s), each with a different central frequency and bandwidth, as used in initial LIGO searches [8]. A fourth waveform, with longer duration and narrow bandwidth, was found incompatible with the **BayesWave** parameters used in this search. An example scatter plot showing the results of white noise burst waveforms with a bandwidth from 50-150 Hz is shown in Figure 8. In the figure, the colorbar shows the network

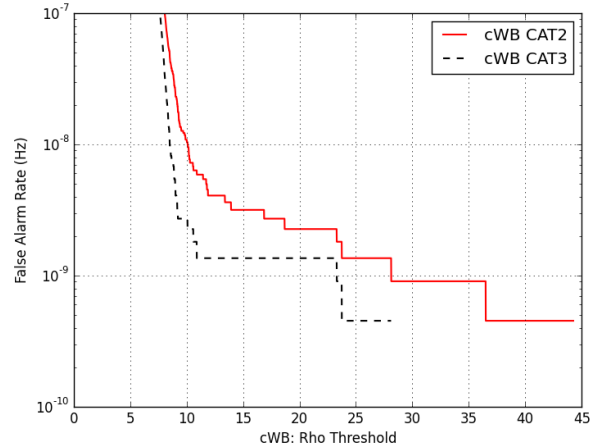


FIG. 7. Background for the **cWB** pipeline using the S6 data used to study ad-hoc signals. The background was calculated using 70 years of time-slide data. The two curves show the background after applications of “Category 2” (red) and “Category 3” (black) data quality vetoes.

SNR, and the X and Y axes correspond to the **cWB** and **BayesWave** detection statistics, respectively. Also shown are the loudest background event after category 2 data quality for both the first stage **cWB** cuts (red, vertical line) and the second stage **BayesWave** ranking statistic (blue, horizontal line). These thresholds divide the figure into four quadrants, representing if the event was detected at various stages of the hierarchical pipeline. For example, events in the upper left quadrant stood above the background for the hierarchical pipeline, but would not have been detected using only the basic version of the **cWB** pipeline. We say these events were “promoted” by the **BayesWave** follow-up, since their detection confidence increased due to this step.

Since  $\rho$  scales linearly with SNR, moving from left to right across the figure represents growing SNR. As the network SNR grows from 10 to 30,  $\log \mathcal{B}_{S,G}$  is seen to grow quickly. This is expected for complex waveforms: signals with higher SNR require more wavelets to reconstruct, as in Equations 1 and 2. Figure 8 shows that the typical event with network SNR  $> 15$  has a bayes factor that exceeds the loudest background event, and so could be detected with high confidence. To reproduce a result like this was not possible using only a basic application of **cWB**; **BayesWave** or some other form of follow-up was required for high confidence detections.

To quantify the performance of the second stage in the hierarchical pipeline, Figure 9 shows the performance of both the hierarchical pipeline and the first stage **cWB** cuts at various FAR thresholds. The efficiency shown on the Y-axis uses the number of triggers identified by **cWB** with network SNR  $< 80$  as the denominator, and shows the fraction of these events recovered above the threshold on the X-axis. The efficiency of recovering events at high

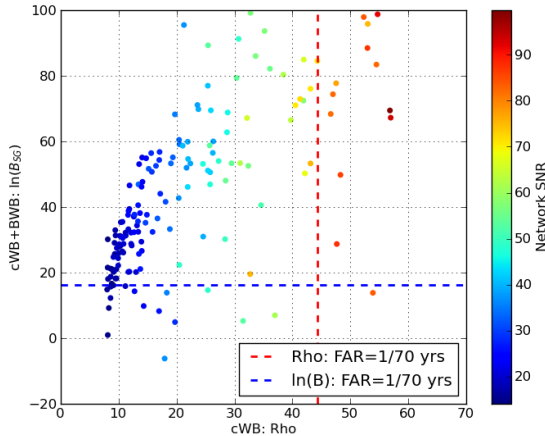


FIG. 8. Scatter plot of white noise burst injections in the 50-150 Hz bandwidth. Events in the top-left quadrant were “promoted” to possible detections by the application of *BayesWave* in the second stage of the hierarchical pipeline.

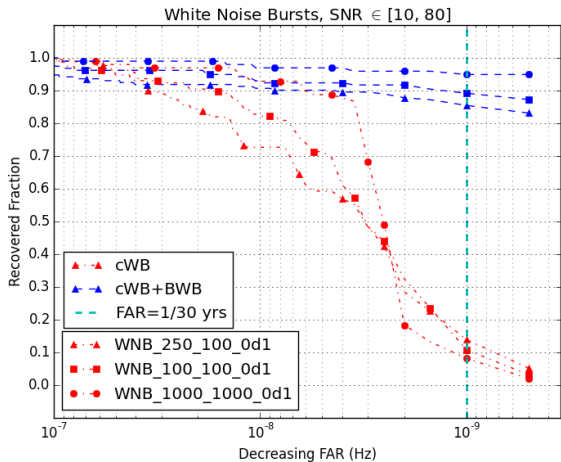


FIG. 9. Fraction of white noise burst injections identified in the first stage which were recovered at various FAR thresholds, after applying CAT 2 vetoes. The right side of the figure indicates higher confidence detections. The hierarchical pipeline performs well recovering complex waveforms at high confidence. For waveform details, see [8].

confidence is seen on the right side of the plot. The second stage of the pipeline “promotes” 80-95% of the events to a FAR < 1/70 years, where essentially none of the events in this SNR range cross this threshold using only the first stage of the pipeline.

#### D. Injections: Sine-gaussians

We also tested a variety of sine-gaussian waveforms with different central frequencies and quality factors. These waveforms match the basis wavelets used by

*BayesWave*, so they have minimal complexity, and in Equation 1,  $N \approx 1$ . This means that  $\log \mathcal{B}_{S,G}$  scales with the logarithm of SNR. This leads to a counter-intuitive conclusion: The most challenging waveforms for *BayesWave* to detect are sine-gaussians, because they match the basis used by the pipeline.

An example of this logarithmic scaling may be seen in Figure 10. Compared with the white noise bursts in Figure 8, the Bayes Factor of the sine-gaussian injections grows very slowly with SNR. The result is that nearly all of the events have  $\log \mathcal{B}_{S,G}$  in the range 5–20. Comparing with the background distribution, we can see this means the hierarchical pipeline will detect most sine-gaussian signals with a FAR  $10^{-10}$ – $10^{-8}$  Hz, or about 1 background event per 3-300 years. This FAR is too low to make first detections, though it may be in the right range for identifying interesting candidates, and may be appropriate in a future scenario where GW detections are common.

The FAR range where *BayesWave* detects sine-gaussian signals loosely corresponds to the FAR levels where we see long tails in the naive cWB background. Moreover, experience with cWB suggests that typical glitch populations that pass basic selection cuts often have a simple time-frequency structure. The statistical framework developed for *BayesWave* predicts this effect: glitches with simple time-frequency structure may appear as coincident in both detectors, and so mimic real signals. However, glitches with complex time-frequency structure are highly unlikely to appear identical in two or more detectors, and so can typically be rejected by testing for signal power inconsistent with the astrophysical model. One could argue the *BayesWave* ranking by signal complexity is a natural approach for this reason: signals with simple time-frequency structure may be plausibly explained as a glitch, while signals with complex time-frequency structure are extremely unlikely to appear consistent with a GW signal in two detectors by chance. The conclusion, then, is that short duration sine-gaussian waveforms represent a special case which are challenging to detect at high confidence due to similarity with detector glitches. The results in Figure 11 show that the hierarchical pipeline and basic cWB perform at a similar level for these waveforms. If nature indeed produces simple waveforms, from sources like cosmic string cusps, very high mass binary black holes, etc., perhaps they can be recovered with more specialized burst searches, or populations of such events could stand above the background.

## V. DISCUSSION

In this work, we introduced a hierarchical pipeline which combines two previously described algorithms for finding GW burst signals. The performance of the hierarchical pipeline was tested using a variety of simulated waveforms embedded in data from the two detector LIGO network. The testing demonstrated that for this data set:

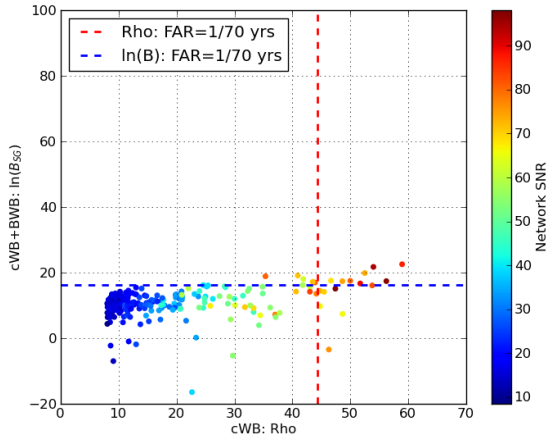


FIG. 10. Scatter plot of 153 Hz, Q9 sine-gaussian injections. The injections have a simple time-frequency structure, so the Bayes Factor scales only weakly with SNR.

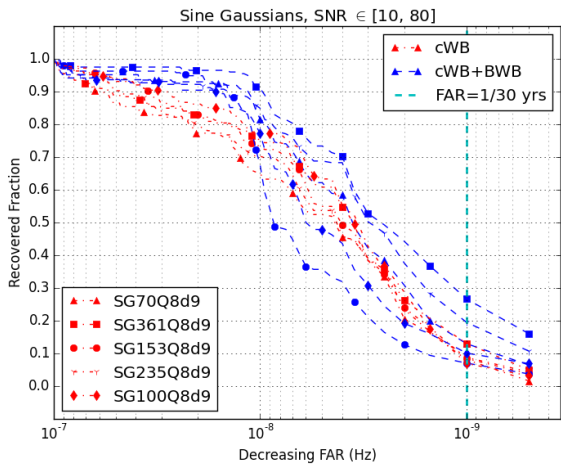


FIG. 11. Fraction of sine-gaussian injections detected at various FAR thresholds. The simple waveforms are detected at low confidence, but not at high confidence. For waveform details, see [8].

- For complex waveforms requiring several wavelets to fit, including white noise bursts and binary black hole merger signals, the hierarchical pipeline can make high confidence detection for low SNR events.
- For simple waveforms (for example, sine-gaussians), the hierarchical pipeline does not improve the detection confidence and other alternative approaches need to be explored.
- The distribution of background events studied with *BayesWave* was broadly consistent with a simple,

predictive model.

The implication for the early Advanced LIGO network is clear: using a detection statistic that accounts for waveform complexity, as was done here with *BayesWave*, enables high-confidence detection of short GW bursts even in the presence of loud glitches.

The fact that *cWB* uses a detection statistic that scales linearly with SNR means that even a single loud glitch in the background set requires special attention to enable high-confidence detections. The *cWB* background typically contains large “tails”, and so follow-up or specialized cuts are required. On the other hand, glitches which contain significant time-frequency structure, and so require multiple wavelets to reconstruct, are extremely unlikely to have the same time-frequency structure in two detectors. *BayesWave* leverages this feature of the data to assign a high detection confidence to signals with complex time-frequency structure, and a low confidence to simple signals. This means that simple, loud glitches are “down-weighted” by *BayesWave*, while complex glitches are most likely rejected due to a lack of coherence between detectors. The fact that *BayesWave* uses this important morphology information to rank events, while *cWB* ranks mainly by coherent SNR, are complimentary features of the two algorithms.

Finally, we note that the strong performance shown here is not necessarily restricted to this particular implementation. Rather, this is a result of a detection statistic that better reflects the properties of LIGO data than SNR based schemes. Such a statistic could be implemented in a less computationally intensive framework, so that a single stage pipeline may show similar performance. In this sense, we hope that this work marks a turning point in the culture of GW transient searches, so that our community can move beyond only looking for the very loudest signals, and instead give proper statistical weight to waveform morphology in our searches.

## VI. ACKNOWLEDGEMENTS

Thank you to Kent Blackburn, Reed Essick, Tjonnie Li, Joey Shapiro Key, Patricia Schmidt, Tiffany Summerscales, Michele Vallisneri, Salvatore Vitale, Leslie Wade, and Alan Weinstein for helpful conversations about this work. Thanks also to Seth Kimbrell and Francesco Pannarale for contributions to *BayesWave* development. LIGO was constructed by the California Institute of Technology and Massachusetts Institute of Technology with funding from the National Science Foundation and operates under cooperative agreement PHY-0757058. T.B.L. acknowledges the support of NSF LIGO grant, award PHY-1307020. This paper carries LIGO Document Number ligo-p1500137-v7.

- 
- [1] J. Aasi, B. P. Abbott, R. Abbott, T. Abbott, M. R. Abernathy, K. Ackley, C. Adams, T. Adams, P. Addesso, *et al.*, *Classical and Quantum Gravity* **32**, 074001 (2015), arXiv:1411.4547 [gr-qc].
- [2] J. Abadie, B. P. Abbott, R. Abbott, M. Abernathy, T. Accadia, *et al.*, *Classical and Quantum Gravity* **27**, 173001 (2010), arXiv:1003.2480 [astro-ph.HE].
- [3] F. Acernese, M. Agathos, K. Agatsuma, D. Aisa, N. Allemandou, A. Allocca, J. Amarni, P. Astone, G. Balestri, G. Ballardín, *et al.*, *Classical and Quantum Gravity* **32**, 024001 (2015), arXiv:1408.3978 [gr-qc].
- [4] H. Grote and the LIGO Scientific Collaboration, *Classical and Quantum Gravity* **27**, 084003 (2010).
- [5] Y. Aso, Y. Michimura, K. Somiya, M. Ando, O. Miyakawa, T. Sekiguchi, D. Tatsumi, and H. Yamamoto, *Phys. Rev. D* **88**, 043007 (2013), arXiv:1306.6747 [gr-qc].
- [6] J. Abadie, B. P. Abbott, R. Abbott, T. D. Abbott, M. Abernathy, T. Accadia, F. Acernese, C. Adams, R. Adhikari, C. Affeldt, and *et al.*, *Phys. Rev. D* **85**, 082002 (2012), arXiv:1111.7314 [gr-qc].
- [7] B. P. Abbott, R. Abbott, R. Adhikari, P. Ajith, B. Allen, G. Allen, R. S. Amin, S. B. Anderson, W. G. Anderson, M. A. Arain, and *et al.*, *Phys. Rev. D* **80**, 102001 (2009), arXiv:0905.0020 [gr-qc].
- [8] J. Abadie, B. P. Abbott, R. Abbott, T. D. Abbott, M. Abernathy, T. Accadia, F. Acernese, C. Adams, R. Adhikari, C. Affeldt, *et al.*, *Phys. Rev. D* **85**, 122007 (2012), arXiv:1202.2788 [gr-qc].
- [9] E. Thrane and M. Coughlin, *ArXiv e-prints* (2015), arXiv:1507.00537 [astro-ph.IM].
- [10] N. J. Cornish and T. B. Littenberg, *Classical and Quantum Gravity* **32**, 135012 (2015), arXiv:1410.3835 [gr-qc].
- [11] S. Klimentenko, I. Yakushin, A. Mercer, and G. Mitselmakher, *Classical and Quantum Gravity* **25**, 114029 (2008), arXiv:0802.3232 [gr-qc].
- [12] T. Littenberg, N. Cornish, J. Kanner, and M. Millhouse, *In Prep* (2015).
- [13] S. Mohapatra, L. Cadonati, S. Caudill, J. Clark, C. Hanna, S. Klimentenko, C. Pankow, R. Vaulin, G. Vedovato, and S. Vitale, *Phys. Rev. D* **90**, 022001 (2014), arXiv:1405.6589 [gr-qc].
- [14] J. Aasi, J. Abadie, B. P. Abbott, R. Abbott, T. D. Abbott, M. Abernathy, T. Accadia, F. Acernese, and *et al.*, *ArXiv e-prints* (2013), arXiv:1304.0670 [gr-qc].
- [15] J. Aasi, J. Abadie, B. P. Abbott, R. Abbott, T. Abbott, M. R. Abernathy, T. Accadia, F. Acernese, C. Adams, T. Adams, and *et al.*, *Classical and Quantum Gravity* **32**, 115012 (2015), arXiv:1410.7764 [gr-qc].
- [16] Y. Pan, A. Buonanno, M. Boyle, L. T. Buchman, L. E. Kidder, H. P. Pfeiffer, and M. A. Scheel, *Phys. Rev. D* **84**, 124052 (2011), arXiv:1106.1021 [gr-qc].
- [17] S. K. Chatterji, *The search for gravitational wave bursts in data from the second LIGO science run*, Ph.D. thesis, Massachusetts Institute of Technology (2005).
- [18] M. Vallisneri, J. Kanner, R. Williams, A. Weinstein, and B. Stephens, *Journal of Physics Conference Series* **610**, 012021 (2015), arXiv:1410.4839 [gr-qc].